RP Materials: Proceedings
Vol. 1, Part 1 (2022) pp. 5–8
e-ISSN:

RESEARCH PLATEAU PUBLISHERS

Cite this article: N. Singh, Micro and nano rheological studies of viscoelastic materials, *RP Materials: Proceedings* Vol. 1, Part 1 (2022) pp. 5–8.

Original Research Article

Micro and nano rheological studies of viscoelastic materials

Navneet Singh
Department of Physics, Rajiv Gandhi Government College for Women, Bhiwani – 127021, Haryana, India
*Corresponding author, E-mail: navneetdhanda16@gmail.com

****Selection and Peer-Review under responsibility of the Scientific Committee of the National Conference on Advanced Engineering Materials (NCAEM 2022).**

ARTICLE HISTORY
Received: 6 Aug. 2022
Revised: 4 Nov. 2022
Accepted: 8 Nov. 2022
Published online: 27 Dec. 2022

KEYWORDS
Nanoparticles; iron oxide; sol-gel; Mossbauer; magnetization.

ABSTRACT
Micro and nanoscale rheological studies provide information on the potential presence of small inhomogeneities in the structure of viscoelastic materials that are often inaccessible using traditional mechanical rheometers. At these length scales, the video microscopy approach enables susceptible capacity of the viscoelastic and viscous media. Investigations are conducted to determine the location of a tracer particle that is embedded in these materials. By using direct video imaging and image analysis tools, it is possible to determine the position of an implanted latex bead in a particular medium and estimate its transient state mean-square displacement. On the basis of this, the viscoelastic material's loss moduli and storage have been computed. In order to calibrate our set-up, we give here the video microscopic findings of rheological experiments in pure viscous liquids like water and glycerol. In order to enable a successive free-bead video investigation, an optical tweezer assists in moving and positioning the bead at preferred place inside a micro-volume of the sample. Also, we explore the polymer networks of regenerated silk fibroins (RSF) from Bombyx mori silk fibres at various concentrations using this calibrated method. It has been demonstrated that the usage of presented method, we are able to identify inhomogeneities, if present, at micro and nanometer length scales, within the frequency range constrained by the video recording frame rate (30 Hz) of our CMOS camera.

1. Introduction

Since many years ago, researchers have looked for hints about the mechanisms behind diverse phenomena in viscoelastic materials in the diffusion and systematic drift of implanted beads in those media. Sheetz et al [1] demonstrated that the mechanical characteristics of bio-materials are directly associated with the biological function. In order to analyse and characterise basic viscoelastic materials, such as polymer networks, gels, foams, biopolymers, etc., conventional macrorheology has proven to be a valuable technique [2]. Mechanical rheometry, a traditional method for characterising these materials, is slow and arduous and needs 5–10 ml of sample. The advantage of microrheology is that it can examine the properties of viscoelastic materials at the micro- and nanoscale, revealing details about their structure and intermolecular interactions [2, 3]. Moreover, this method only needs a few tens of microliters of sample for analysis. To analyse viscoelastic materials, various micro-rheological methods have been build up in the past [2, 3]. One such technology for examining the rheological characteristics of simple and visco-elastic media at micro and nanoscale is video microscopy [4]. To calibrate our device, we employed pure viscous substances like glycerol and water. This calibrated system is used to research the rheological characteristics of a biopolymer visco-elastic material, named "regenerated silk fibroin" (RSF).

2. Video microscopy

While using video microscopy to examine a sample's rheological characteristics, the (temporal-line up) image borders of implanted beads are processed. As stated in the literature [5], the sample is magnified in our setup using a 100X oil immersion objective, and then viewed with the help of a display unit. The frame rate of the display unit; for our system is 30 f.p.s. (640×480 pixels) or 15 f.p.s. (1280×1024), determines the time-dependent resolution of display microscope. Optical magnification and CMOS pixel density determine the phase-space resolution of display microscope [4, 6]. In case of border speed of 15 f.p.s., it is recorded as 58 per pixle, whereas in case of border speed of 30 f.p.s., it is recorded as 182 nm per pixle. While diffraction prevents optical assessments of particle size, image analysis tools can pinpoint the location of a single particle with sub-pixel accuracy [4]. On a computer's hard drive, clips of bead's zig-zag path in a particular material have been kept (Intel Core i5, 1 TB RAM, 1 TB HDD). The positions of the beads in each frame are then analysed using image analysis methods. With the adjustment of intensity peaks into the Gaussian profile, these methods can locate beads [4]. This method necessitates an additional step of appropriately connecting the features between the photos if several features are recorded. The feature finding technique that we employed in this work was first created by Crocker and Grier [4] and later included in IDLVM (freely available on the internet) by Ryan Smith. With an

accuracy of a few tens of nanometers [4, 6], this programme can identify bead displacements in a series of image frames. With careful adjustment of microscope high on top of (approximately 28 µm) the cover-slip wall to prevent some potential contact between cover-slip and beads, over 1000 pictures are recorded for each measurement. The beads are moved and located to this target site using an optical tweezer [5]. We can track several beads (3-5) at once using video microscopy. Its multiple particle tracking speeds up the process of obtaining accurate data statistics while helping to determine the positions of a large number of beads.

3. Methodology

We may determine the temporal Mean Square Displacement (MSD = $\left\langle \Delta\vec{r}^{\,2}(\tau)\right\rangle$) of temperature controlled bead in the specified material at the particular temperature T by using the information about its position over time, which is defined as [2, 3]:

$$\left\langle \Delta\vec{r}^{\,2}(\tau)\right\rangle = \left\langle \left|\vec{r}(t)+\vec{r}(\tau+t)\right|^2 \right\rangle, \quad (1)$$

In equation (1), the average is determined at each beginning time t, and τ is the lag time.

Equation (1) is used in custom programmes created in the LabVIEW platform to determine the temporal mean square displacement by utilizing the unprocessed data. By the generalised Stokes-Einstein relation (GSER) provided by [7], this mean square displacement for the said material is connected to modulus of rigidity $G^*(s)$ in the Laplacian regime.

$$\left\langle \Delta r^2(s)\right\rangle = \frac{k_B T}{\pi a s G^*(s)}. \quad (2)$$

In equation (2), k_B stands for the Boltzmann constant, s is the Laplace frequency and other symbols have their usual meaning.

A reliable theoretical groundwork for the GSER was supplied by Levine and Lubensky [8], via which one can determine the frequency range (10-10^7 Hz) across which accurate evaluation of rheological characteristics of colloidal samples is valid [2]. In order to get the modulus of rigidity $G^*(\omega)$ in the Fourier domain, the storage and attenuated modulus ($G'(\omega)$ and $G''(\omega)$) from mean square displacement value, the author employed the estimate approach [9, 10].

$$G'(\omega) = \frac{G^*(\omega)}{1+\beta'(\omega)}.\cos\left[\frac{\pi\alpha'(\omega)}{2} - \beta'(\omega)\alpha'(\omega)\left(\frac{\pi}{2}-1\right)\right], \quad (3)$$

$$G''(\omega) = \frac{G^*(\omega)}{1+\beta'(\omega)}.\sin\left[\frac{\pi\alpha'(\omega)}{2} - \beta'(\omega)[1-\alpha'(\omega)]\left(\frac{\pi}{2}-1\right)\right], \quad (4)$$

and

$$G^*(\omega) = \frac{k_B T}{\pi a\left\langle \Delta r^2(1/\omega)\right\rangle \Gamma[1+\alpha(\omega)][1+\beta(\omega)/2]}. \quad (5)$$

4. Sample preparation

According to descriptions in the literature [11], multivoltain silk fibres from Bombyx mori silk worms are used to renew silk fibre solutions. In $Ca(NO_3)_2$ $4H_2O$ CH_3OH solution, this polymer solution creates networks of regenerated silk fibroins (RSF) [11, 12]. This technique makes use of silk fibres that have been degummed from hydrophilic coat proteins (sericins). RSF solutions with concentrations of 1.00%, 0.50%, and 0.15% have been produced. To prevent inter-bead molecular interaction, the polystyrene beads (Cat# 07310-15, 0.983 µm,) used as probes were introduced to samples at low concentrations. In both simples and viscoelastic materials, these small probe particles are utilised to estimate the relationship between deformation and stress. Each trial utilised about 70 µl of sample, which was carefully placed inside the microscope's slides and sealed via a #1 quality covered coating to prevent air and moisture from entering the material.

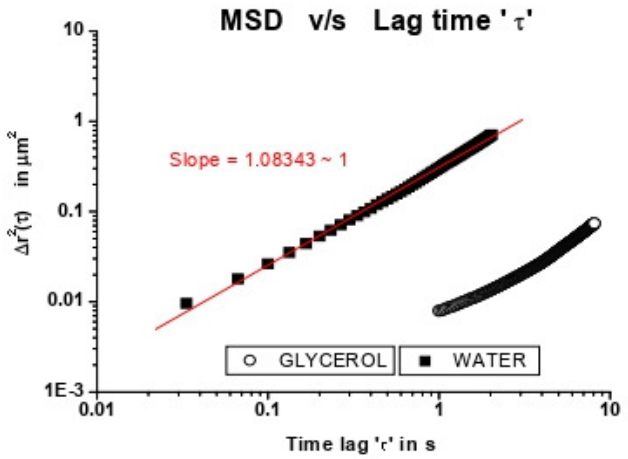

Figure 1: MSD of glycerol and water.

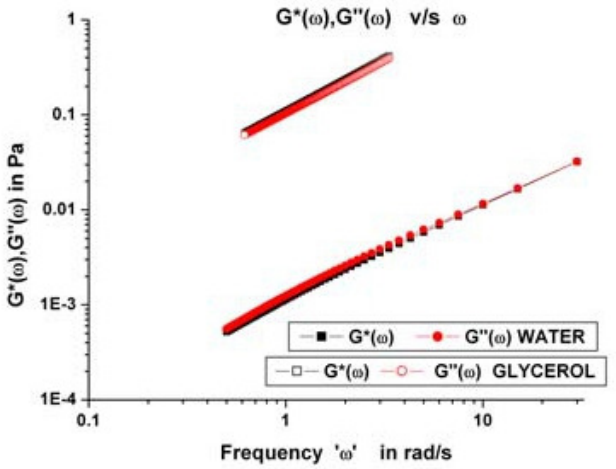

Figure 2: Moduli of glycerol and water.

Initially, the author has employed 0.983 µm beads made up of polystyrene material in purely sticky fluid like glycerol and water to test and calibrate our set up. We used equation to get mean square displacement of beads in both the aqueous media based on the location data (Eq. 1). With relation to lag time, Figure 1 depicts the measured MSD of water (solid square) and glycerol (open circle), respectively. The MSD

value shown in Figure 1 is the ensemble average of measurements made with 10–12 beads at various locations throughout the sample. According to the aforementioned description, the loss modulus of the water and glycerol is estimated using this MSD value. It is further evidence that the media are pure viscous in nature as slope of mean square displacement with respect to τ plot is virtually one (Figure 1) [6, 9]. For glycerol, take note that the MSD values below 60 nm [2] are not included because they cannot be correctly resolved by our system. Equation (3) yields the shear modulus and loss modulus, which are displayed in Figure 2 for the two fluids. Since they are made of only viscous materials, the storage moduli vanish for all acceptable values of frequency. According to this relationship, the loss modulus shows a linear variation with the frequency as:

$$G''(\omega) = \eta\omega. \tag{6}$$

Figure 2's slope can be used to compute the viscosity by fitting log (G"(ω)) to log (η) + log (ω). According to this fitting, the viscosities of glycerol and water have been obtained as: 0.890 ± 0.059 Pa-s and 1.09 ± 0.03 m Pa-s, respectively. These findings and the benchmark values are in strong agreement. This allows us to adjust our configuration. This calibrated setup has been utilised by us to research RSF solutions. The previously described approach is used to obtain The outfit had an average MSD of 15–18 beads for each RSF solution concentration. A bead's MSD behaviour in RSF at varied concentrations and lag time is shown in Figure 3. This plot contains various slopes (between 0 and 1) at various lagging intervals. This nonlinear response of MSD with lag time suggests that the solution for silk fibres has properties that are both elastic and viscous.

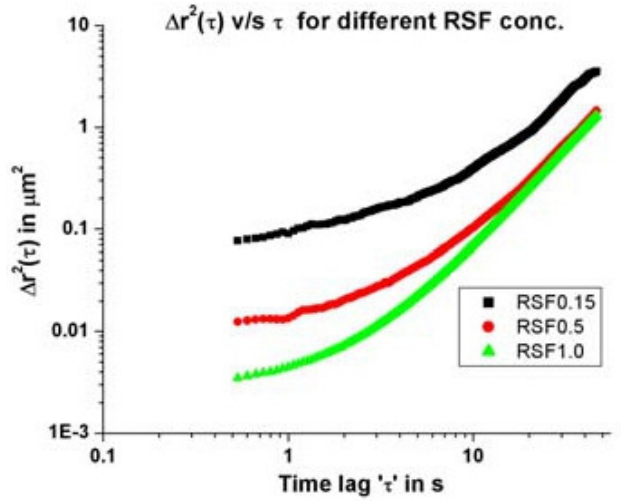

Figure 3: MSD for different RSF concentration.

Figure 4 illustrates the shear moduli (moduli of rigidity) for different RSF concentration. The amount of modulus of rigidity grows as the RSF solution's concentration in $Ca(NO_3)_2$ CH_3OH $4H_2O$ increases. At low frequencies, the material behaves like a fluid, and at high frequencies, like a solid. For various samples, the crossover frequency varies, and its value rises with RSF solution concentration.

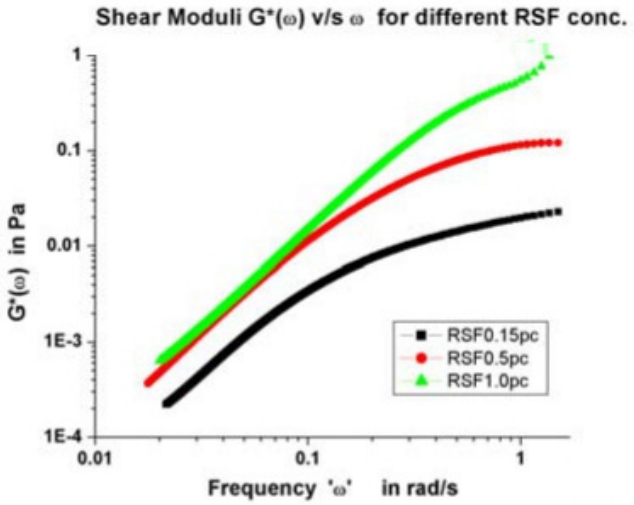

Figure 4: Shear moduli for different RSF concentration.

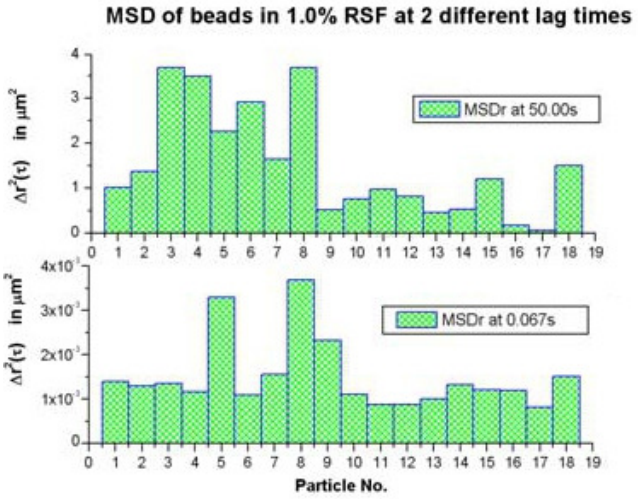

Figure 5: MSD of different beads in 1.0% RSF solution at two lag times 0.067s and 50.0s showing 2 different family of population. One with more MSD (> 1 μm^2) and other with less MSD.

Examining the MSD distribution of beads in a 1.0% RSF solution at various lag times reveals intriguing RSF solution phenomena. Figure 5 displays 18 bead MSD readings at two time lags of 0.067 s and 50.0 s. The MSD distribution is nearly uniform for short lag times. The consistency of the MSD values of 18 beads degrades with increasing lag time (data not shown). Two different families of MSD values start to occur with lag times of 40.0 s and higher. One family of beads displays an MSD value larger than 1 μm^2 during a lag period of 50.0 s, while the other family displays an MSD value less than 1 μm^2. This demonstrates the RSF solution's heterogeneity. Beads' lower MSD values can be attributable to the sample's inclusion of cages, which trap the beads and cause restricted diffusion. Some beads exhibit highly unrestricted diffusion in the sample and, as a result, exhibit comparatively high MSD values. Figures 6 and 7 illustrate how these two families' rheological properties differ when they are divided and averaged independently.

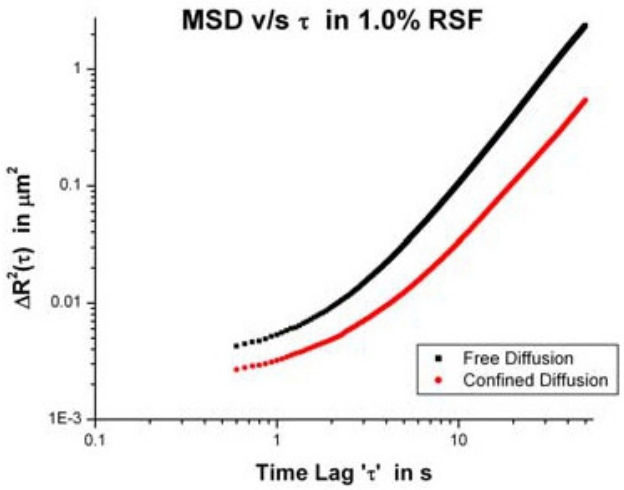

Figure 6: MSD for two different families.

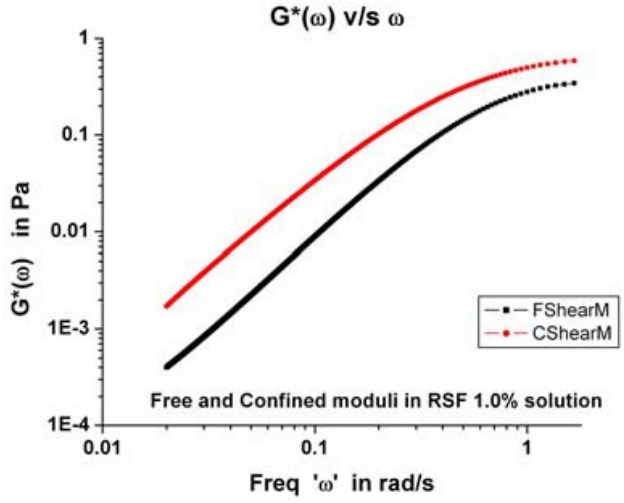

Figure 7: Shear moduli for two different families.

The two forms of MSD values for beads are present in the same 1.0% RSF solution, as shown in Figure 6. Low MSD bead populations exhibit high shear moduli, and vice versa (Figure 7).

5. Conclusions

The aforementioned findings show that video microscopy is an effective method for studying rheology at the micro and nanoscales. We have demonstrated the variability of the RSF polymer solution using video microscopic method. To better understand the rheology of RSF solution under various physical and chemical circumstances, more research, which is currently being done, is required.

References

[1] M. Sheetz, S. Turney, H. Qian, Nanometre level analysis demonstrates that lipid flow does not drive membrane glycoprotein movements, *Nature* **340** (1989) 284-288.

[2] T.A. Waigh, Microrheology of complex fluids, *Rep. Prog. Phys*. **68** (2005) 685-742.

[3] M.L. Gardel, M.T. Valentine, D.A. Weitz, *Microscale Diagnostic Techniques, Microrheology,* Springer, Verlag (2005).

[4] J.C. Crocker, D.G. Grier, Methods of digital video microscopy for colloidal studies, *J. Colloid Interface. Sci*. **179** (1996) 298-310.

[5] A. Raghu. S. Ananthamurthy, Construction of an optical tweezer for nanometre scale rheology, *Pramana J. Phys*. **65** (2005) 699-705.

[6] V. Breedveld, D.J. Pine, Microrheology as a tool for high-throughput screening, *J. Mater. Sci*. **38** (2003) 4461-4470.

[7] T.G. Mason, D.A. Weitz, Optical measurements of frequency dependent linear viscoelastic moduli of complex fluids, *Phys. Rev. Lett*. **74** (1995) 1250-1253.

[8] A. Levine, T.C. Lubensky, One- and two-particle microrheology, *Phys. Rev. Lett*. **85** (2000) 1774-1777.

[9] T.G. Mason, Estimating the viscoelastic moduli of complex fluids using generalized Stokes-Einstein equation, *Rheol. Acta*. **39** (2000) 371-378.

[10] B.R. Dasgupta, S.Y. Tee, J.C. Crocker, B.J. Frisken, D.A. Weitz, Microrheology of polyethylene oxide using diffusing wave spectroscopy and single scattering, *Phys. Rev. E* **65** (2002) 051505.

[11] X. Chen, D.P. Knight, Z. Shao, F. Vollrath,, Regenerated bombyx silk solutions studies with rheometry and FTIR, *Polymer* **42** (2001) 9969-9974.

[12] A. Ochi, Rheology and dynamic light scattering of silk fibrion solution extracted from the middle division of vombyx mori silkworm, *Biomacromolecules* **3** (2002) 1187-1192.